

The ARMA Concept: Comparison of AESA and ARMA technologies for agile antenna design

B. Jecko, IEEE Member, E. Arnaud, XLIM, SYSTEMES-RF Equip. Antennes & Signaux - UMR CNRS n°7252, Limoges University, 87000 Limoges France, H. Abou Taam, A. Siblini, Doctoral School of Science and Technology, Lebanese University, Lebanon

Abstract—This paper compares two solutions for designing electronically agile beam antennas: the well-known AESA (Agile Electronically Scanned Arrays) approach and a new one called ARMA (Agile Radiating Matrix Antenna) [1]. This comparison is performed first on the electromagnetic principles of the two methods, and secondly on the performances in terms of bandwidth, radiation efficiency, coupling effects, side lobes, agility in beam forming and beam steering. Finally a validation of the new approach is performed by comparison of theoretical and experimental results.

Index Terms— Agile Beam Antenna, Beam Forming, Beam Steering, Agile Radiating Matrix Antenna

Electronically agile beam antennas are extensively used today to perform beam forming, beam steering, pattern reconfiguration, multi-sectorial beams, tracking etc. For a long time agile beams are obtained using arrays (AESA) of antennas, with a lot of limitations in terms of radiation efficiency, coupling effects, side lobes, back radiation and so one.

I. ELECTROMAGNETIC APPROACHES COMPARISON

The radiation pattern of any antenna is obtained by using Maxwell Equations; equations of propagation in free space; free space Green function, and applying the equivalent principle on a radiating surface surrounding the antenna. Fig. 1 shows the principle scheme.

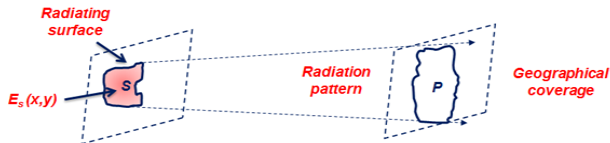


Fig.1 Radiation pattern directly obtained from the radiating surface.

Then the radiated EM field $\vec{E}(P)$ is obtained by a radiating integral like:

$$\vec{E}(P) = \frac{jk}{4\pi} \Psi(R)(1 + \cos\theta)(\cos\phi\vec{e}_\theta - \sin\phi\vec{e}_\phi)SFT. \quad (1)$$

$$SFT = \iint E_s(x,y) e^{j(k_x x \sin\theta \cos\phi + k_y y \sin\theta \sin\phi)} ds. \quad (2)$$

$$\text{With : } \Psi(R) = \frac{e^{jkR}}{R}$$

This integral relates the radiated electromagnetic field $E(P)$ to the field $E_s(x,y)$ on the radiating surface S , as a quasi-Spatial Fourier Transform (SFT).

A moving radiation pattern is obtained by changing the electric field law $E_s(x,y)$ on the radiating surface as shown in figure2.

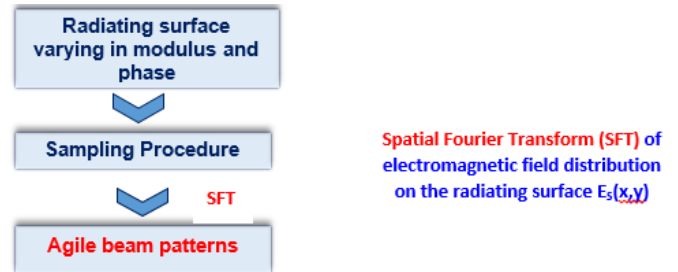


Fig. 2 Agile beam patterns related to radiating surface.

To perform that, the $E_s(x,y)$ field must be sampled, here begins the main difference between the two methods:

II.1 - Sampling using a Dirac function Comb:

This well-known procedure [5] multiplies the $E_s(x,y)$ by a two dimensions Dirac Comb to obtain the sampled following form :

$$\widetilde{E}_s(x,y) = \sum_i \sum_j E_s(x_i, y_j) \delta_{x_i, y_i}(x,y) \quad (3)$$

Where δ is the two dimensions Dirac function characterized by:

$$\int f(x,y) \delta_{x_i, y_j} dx dy = f(x_i, y_j) \quad (4)$$

The $\widetilde{E}_s(x,y)$ sampled field is introduced in the equation (3) and the property of the Dirac function is applied to obtain:

$$E(P) = K \iint_S \sum_i \sum_j E_s(x_i, y_j) \delta_{x_i, y_j}(x,y) e^{j(k_x x \sin\theta \cos\phi + k_y y \sin\theta \sin\phi)} dx dy$$

$$E(P) = K \sum_i \sum_j \iint_S E_s(x_i, y_j) \delta_{x_i, y_j}(x,y) e^{j(k_x x \sin\theta \cos\phi + k_y y \sin\theta \sin\phi)} dx dy$$

Then the electric radiated field appears as a sum of contributions of punctual elementary antennas periodically distributed on the surface S . That is the Array Approach.

II.2 - Sampling by using a rectangular function (quantification) :

If the radiating surface S is sampled into small jointed pieces $s_{i,j}$ called pixels, the radiated electric field is the sum of all these uniform surface field contributions:

$$\vec{E}(p) = k \iint_S E_s(x, y) e^{j(k_x \cdot x \cdot \sin\theta \cdot \cos\phi + k_y \cdot y \cdot \sin\theta \cdot \sin\phi)} ds.$$

$$\vec{E}(p) = k \sum_i \sum_j \iint_{s_{i,j}} E_{i,j}(x, y) e^{j(k_x \cdot x \cdot \sin\theta \cdot \cos\phi + k_y \cdot y \cdot \sin\theta \cdot \sin\phi)} ds.$$

$$\vec{E}(p) = k \sum_i \sum_j \int \int_{s_{i,j}} \overset{\text{weight}}{A_{i,j}} e_{i,j}(x, y) e^{j(k_x \cdot x \cdot \sin\theta \cdot \cos\phi + k_y \cdot y \cdot \sin\theta \cdot \sin\phi)} ds$$

$$= k \sum_i \sum_j A_{i,j} \int \int_{s_{i,j}} e_{i,j}(x, y) e^{j(k_x \cdot x \cdot \sin\theta \cdot \cos\phi + k_y \cdot y \cdot \sin\theta \cdot \sin\phi)} ds.$$

$\alpha_{i,j}$

Fig. 3 Principle of weighting the surface sampled electric field.

Where $e_{i,j}$ and $A_{i,j}$ are respectively: the field on the small surfaces considered as a constant field and the weight applied on each normalized pixel surface field $e_{i,j}$.

This formulation suggests that the whole structure can be considered as a matrix of (M, N) pixels, each able to generate a given contribution to the building of the whole field $E(P)$. In the most general cases, there are no restriction on the surface S , and the pixels can have any shape, but must be connected together. Like for the arrays, the pixels must be fed by a beam forming network (BFN) to apply appropriate weights in order to obtain an expected radiation pattern.

A very important case is to consider low Profile Antennas. For such structures the surrounding surface (fig. 1) is a planar one which can be sampled by pixels with a square $s_{i,j}$ radiating surface, as shown in figure 3a.

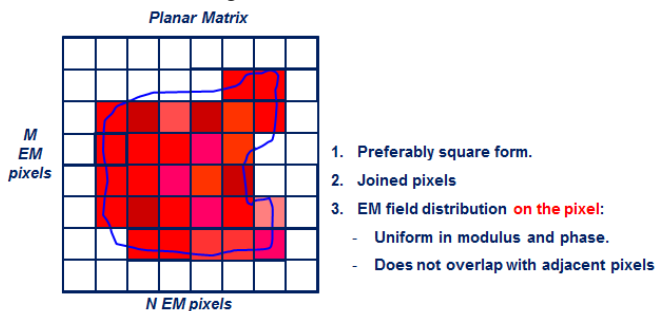


Fig. 3a Radiating surface sampled by jointed square pixels.

The most important point in ARMA approach is to be able to design a pixel which can generate a uniform EM field on its surface. This technic was extensively developed and validated in many papers [1] [2] [4] [6] and it is the key point of the ARMA solution. The corresponding matrix may have many shapes as shown in the figure 3b: 1D planar matrix, 2D planar matrix, conformal matrix...

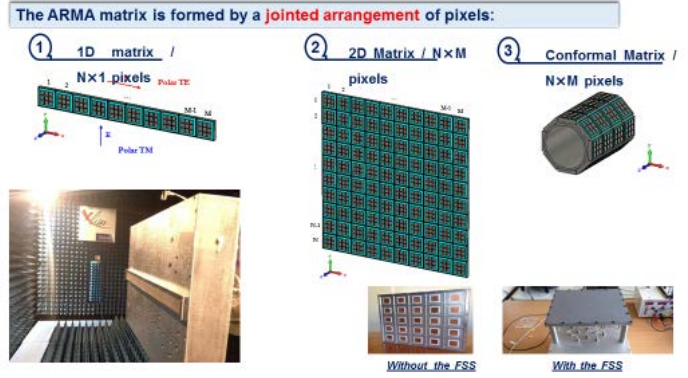


Fig. 3b ARMA Matrix Architectures.

In conclusion, the two approaches introduce different spatial Fourier transform due to the different sampling procedures of the radiating surface. Consequently the properties of these two kind of antennas: ARMA and AESA, are sometimes quite different.

II. COMPARISON OF THE MAIN PROPERTIES OF THE TWO AGILE ANTENNAS: ARMA AND AESA

Let us consider the two kinds of 1D antennas [1], [2], [7] with the same planar surface, the same number of elements (number of elementary array antennas equal to the number of pixels), and the same law of weights for the feeding network (figure 4)

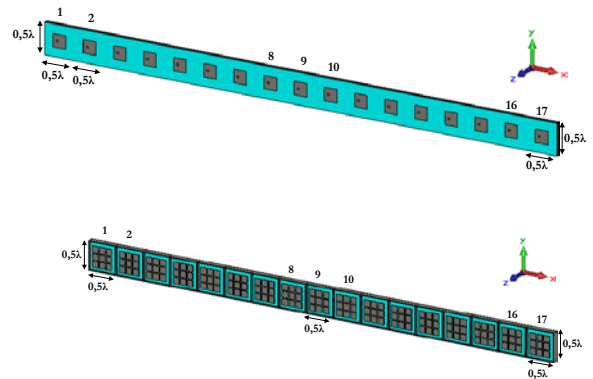


Fig. 4 1D Antennas used to compare the AESA and ARMA approaches.

III.1 - Radiating surface efficiency in the axial direction:

The result of the comparison of the surface efficiencies is the same as comparing a phased array and an aperture antenna (horn antenna for example). In the phased array, the surface efficiency is usually less than 65% and in the horn antenna it is more than 75%. These results are approximately the same with AESA and ARMA respectively. That means a difference in axial gain of 0.6 dB in our example which is not very significant.

It is more significant (2dB) for a larger surface as shown later on the figure 8.

This use of this work is restricted solely for academic purposes. The author of this work owns the copyright and no reproduction in any form is permitted without written permission by the author.

III.2 - Coupling between two adjacent elements:

The coupling effect between two adjacent pixels in ARMA is lower (at least 4 dB) than that one between adjacent elements in the array antenna. This property is due to the radially vanishing mode of the EBG antenna used to build the pixel [8] and not due to the presence of the walls as it is shown clearly in figure 5 where a comparison was made based on three designs working at 8 GHz [7]: an array of 17 patches (fig 4), a one dimensional ARMA of 17 pixels (fig 4) and a 17 elements cavity-backed patch array.

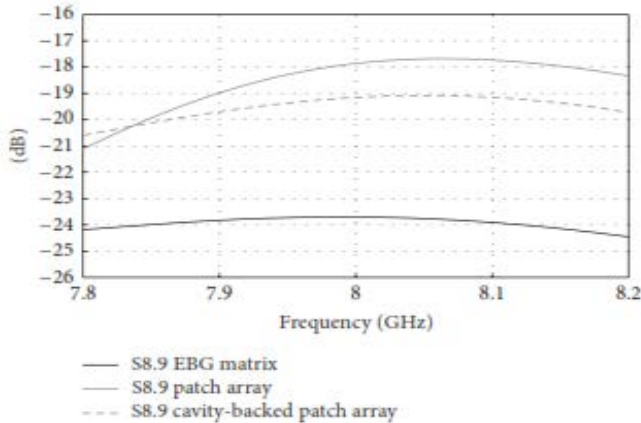


Fig. 5 Coupling coefficient between the 8th and the 9th elements in an ARMA Matrix, a patch array and cavity-backed patch array.

III.3 - Maximum gain as a function of the elevation angle θ

The maximum gain curve must follow the law : $1 + \cos \theta$ (cf : eq 1). That is approximately the case on fig 6 for the ARMA solution but not the case for the patch array for $\theta \geq 55^\circ$ [2].

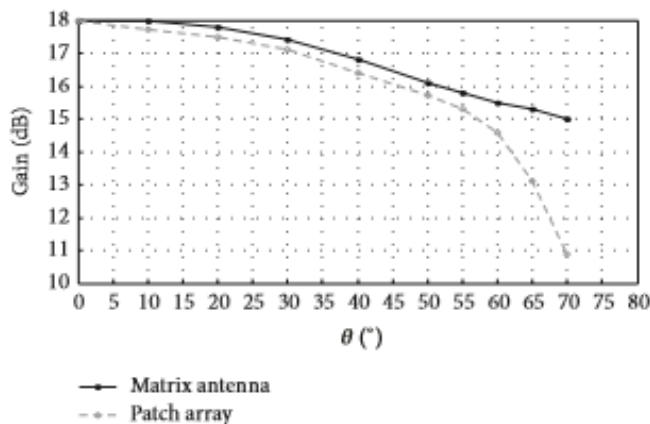


Fig. 6 - Evolution of the gain value versus the scanning angle.

This result is confirmed on the figure n°7 where the maximum of the gain for the 70° direction, is 4 dB higher with ARMA than with AESA.

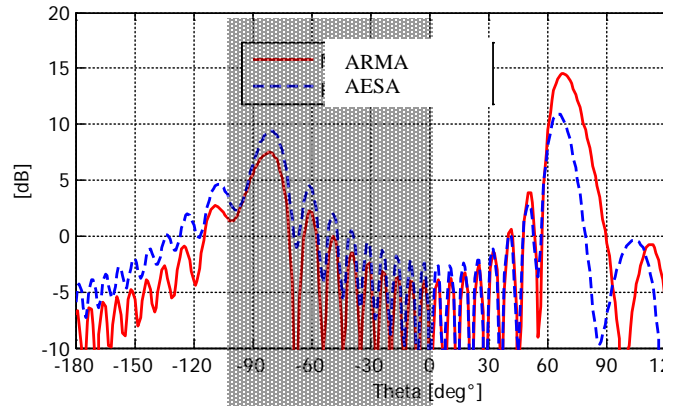


Fig. 7 - Comparison of AESA and ARMA radiation patterns for a beam steering procedure in the 70° direction.

This result can be generalized for any ARMA Antenna used for beamforming [9] or beam-steering with any beam shape [6].

III.4 - Side lobes : Grating lobes compared to pixel lobes.

As it was shown in the first part, the radiated field is approximately the spatial Fourier transform of the sampled surface field and the sampling procedures are different for the ARMA and AESA approaches (cf §I). Since in ARMA procedure the sampled surface field is smoother (uniform sampled surfaces), the spatial Fourier transform introduces lower side lobes [5] as shown in the fig 7 where the grating lobes for the array and pixel lobes for ARMA appear for the same angle (Fourier transforms with the same periodicity) but not at the same level.

Consequently the sampling step for ARMA approach is not limited to 0.8λ for an axial beam antenna and it is possible without significant damages on the radiation pattern to use pixel dimensions up to 1.5λ [7] then a larger periodicity.

Figure 8 shows the comparison of the grating lobes of 1D ARMA of five pixels and that of 1x5 patch array (1.2λ is the dimension of each pixel and also the patch antenna step). A reduce of 11 dB in the grating lobes is obtained in ARMA with a better gain for the main lobe.

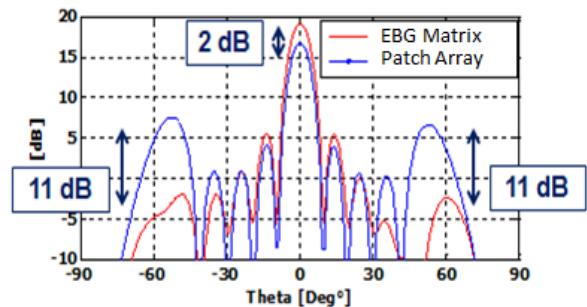


Fig. 8 - Main and grating lobes comparison for 1x5 ARMA matrix and 1x5 patch array with $1.2\lambda \times 1.2\lambda$ periodicity.

III.5 - High axial gain solutions.

In the same way, ARMA and AESA approaches are good choices to obtain high gain (>30dB) with low profile antennas. Unfortunately high gain means a large number of elements which increases dramatically the BFN losses and the cost.

But, as it is shown in the previous paragraph, ARMA is the good candidate to minimize the number of elements of the BFN because the dimensions of the pixels can be increased without significant side lobes effects for a radiation maximum around the axial direction [7].

For example, to obtain a 25 dB gain using an array solution with inter-element steps of 0.6λ , 100 elements need to be use. In the ARMA solution, if the pixel surface of $0.6\lambda \times 0.6\lambda$ is chosen to keep the same periodicity, the ARMA solution needs the same number of elements .But, it is possible to obtain the same results with $1.2\lambda \times 1.2\lambda$ pixels, corresponding to the same radiating surface and the same gain obtained using 25 elements instead of 100, without significant degradation of the pattern. Figure 9 shows the idea of the reduction of the number of elements for the same antenna surface.

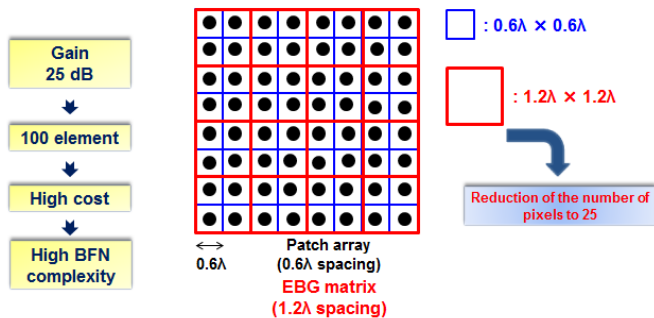


Fig. 9 -Reduction of the number of elements using large pixel dimensions in the ARMA Approach.

To verify this property, a 5*5 pixels ARMA antenna was studied:

The expected directivity (25dB) was obtained with an equi-amplitude and equi-phase feeding procedure (fig: 10, black curve). It is also possible ,like in an array, to introduce a more efficient ponderation law to minimize the side lobes effect (fig: 10 red curve) but it is important to notice that, (like in an array), it is not usually possible to decrease the pixels lobe level located near 50° by this way.

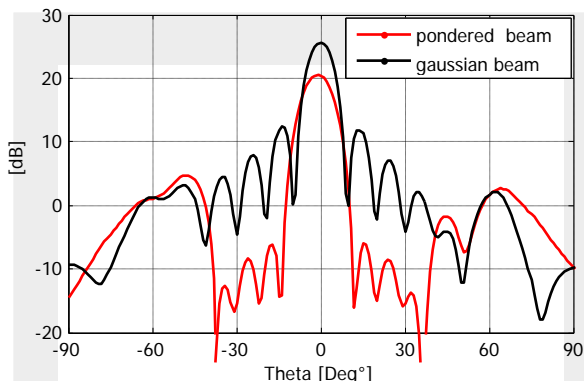


Fig. 10 Axial beam directivity pattern obtained with a 25 pixels antenna.

A second limitation of the ARMA solution with large pixels is shown on the 11th figure. For a small shift from the axial direction ($\theta = 10^\circ$) the pixels lobes already appear. Of course this phenomenon is worse (fig 11) with an array having the same periodicity. This effect can be interpreted by a too large quantification step due to the large dimension of the pixel which affects the spatial Fourier transform.

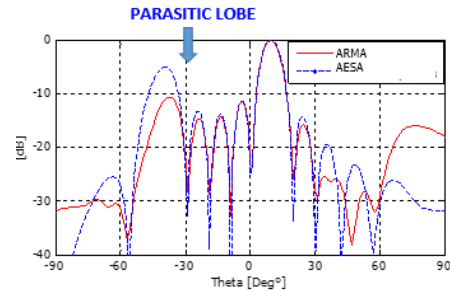


Fig. 11 Comparison between ARMA solution and a patch Array one to have a maximum of the directivity for the 10° elevation angle.

This large pixels ARMA Antenna was manufactured (cf: §III-fig 19) to validate all the results.

III.6 – Frequency dependence

The pixel of the ARMA solution is derived from a low profile EBG Antenna [8] [12] which presents a very stable behavior as a function of the frequency. Consequently the pixel and then the whole ARMA Antenna have the same frequency stability as shown on the directivity maximum as a function of the frequency (fig 12) for the previous example presented on the figure n° 19.

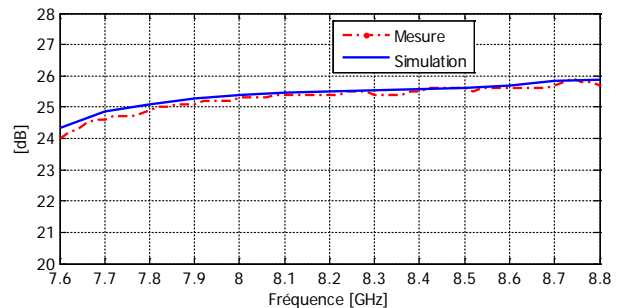


Fig. 12 - Directivity maximum as a function of the frequency

In the same direction, the radiation pattern results for a shifted sectorial beam [6] obtained with the 1×17 pixels antenna (fig: 4) are also very close for different frequencies on the band, as shown on the following pictures (fig 13):

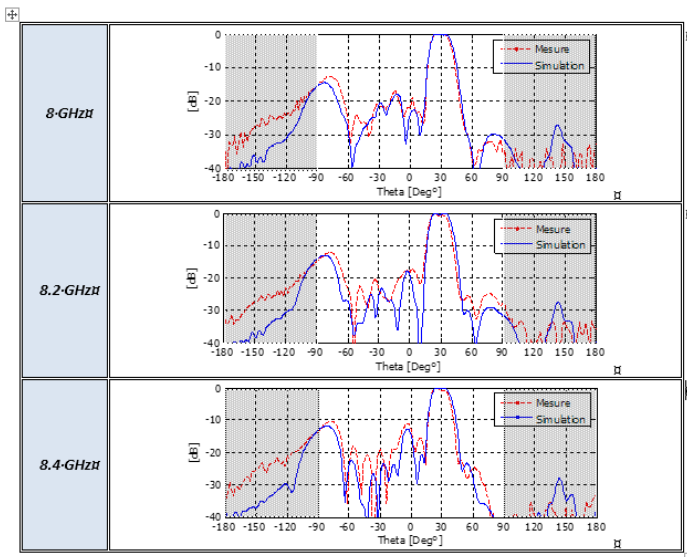


Fig. 13 Theoretical and experimental sectorial beam radiation patterns comparison for three frequencies .Beam steering in the 30° direction.

A bandwidth comparison of the two approaches AESA and ARMA was performed on the previous example (fig 4).The results on the maximum directivity evolution as a function of the frequency show a large difference (more than a “2” factor) This property, already obtained with low profile EBG antennas [8], is easy to extend to any antennas comparison.

III.7 - Wave polarisation : linear, circular, cross-polar..

Like for the frequency behavior, the polarization performances of ARMA depend on these ones of the original EBG antenna which are usually very good with a performant feeding circuit [9]. For example, the axial ratio obtained with a pixel considered alone and fed by a 3 hybrid couplers circuit, is presented on the 14th figure.

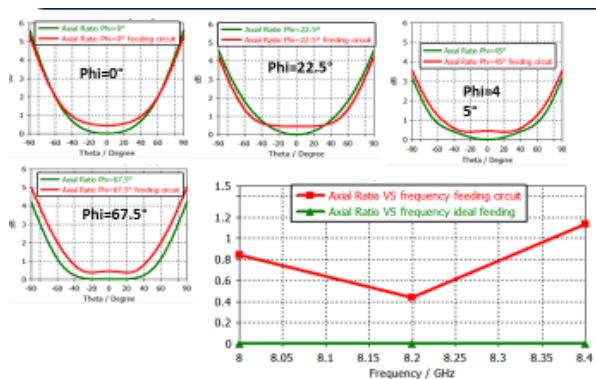
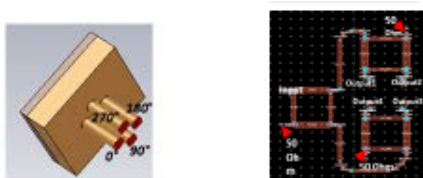


Fig. 14 Space Axial Ratio Evolution and frequency dependence for a pixel fed by a 3 hybrid couplers polarization circuit. Comparison with the deal feeding procedure (green curves).

The results on the space evolution of the axial ratio are very good except for a large radiation angles ($\cong 90^\circ$). This edge phenomenon is minimized when the pixel is considered inside the matrix because, in this case, pixels are joined pixels.

III. EXPERIMENTAL ARMA ANTENNAS MANUFACTURED FOR SOME APPLICATIONS :

IV.1 - Area scanning

To scan a large outdoor area, a 1D matrix with 17 pixels able to cover a large azimuthal surface was manufactured (fig 15 and 16) at 8.2 GHz following the architecture given on the 4th figure.

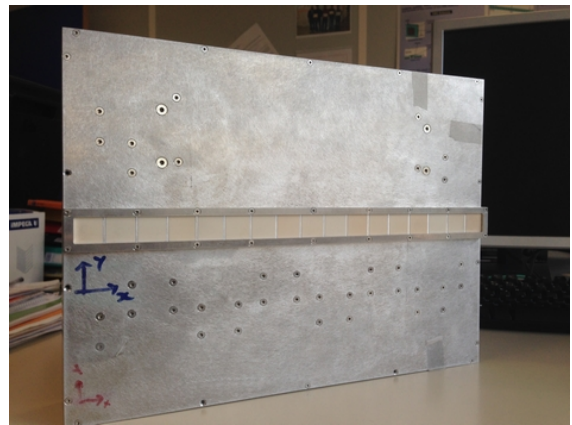


Fig. 15

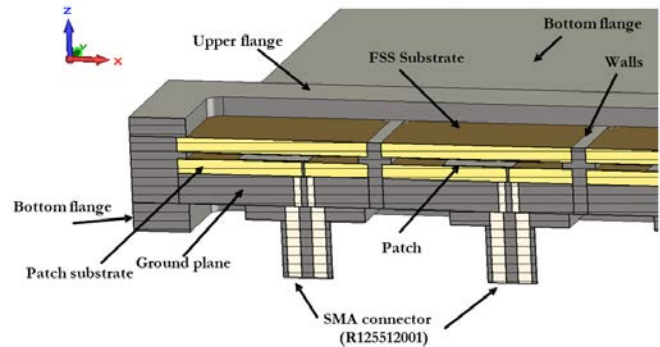


Fig 16 Feeding procedure illustration.

As it was shown on figures 12 and 13 theoretical and experimental results are in good agreement even building a Gaussian beam than a sectorial one [6].

IV.2 – Animal tracking [10] [11]

In our rural region it is important to know where race horses are located in the country side. An ARMA antenna was built in S band to track tagged animals. It use 11 beams with side lobes lower than -20dB to cover a -50° to $+50^\circ$ area. Because the lateral dimension of the antenna was limited, only a nine pixels 1D matrix was manufactured. The whole fabrication procedure is presented on the 17th figure which shows the manufactured

equipment. Also for this application, the experimentally generated beams were in good agreement with the simulated ones (fig. 18).

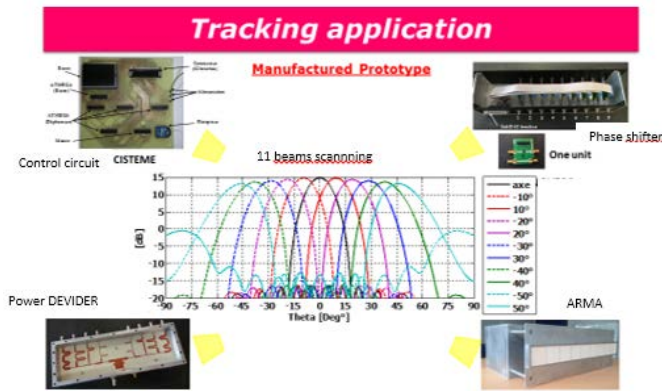


Fig. 17 Whole equipment for a 11 beams scanning.

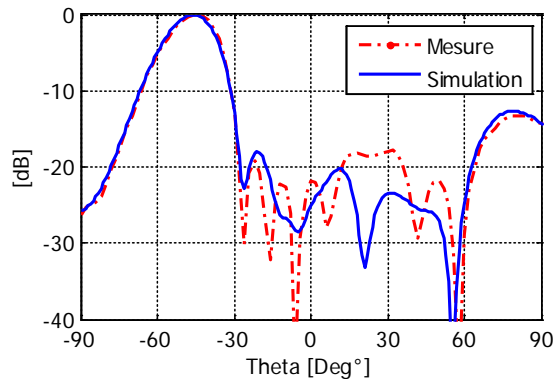


Fig. 18 Theoretical and experimental comparison of a radiated beam in the 50° directions.

IV.3 – Axial high gain applications.

In the case of telecommunications applications, very high gains are expected: higher than 30dB .But because of the price just a 25dB gain antenna was built to day; the prototype is shown on the 19th figure.

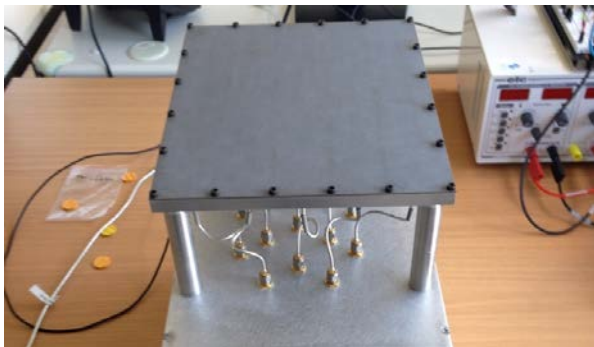


Fig. 19 Final prototype of a 5 x 5 pixels matrix.

- The realized gain, obtained by both a theoretical and an experimental approach don't move very much with the frequency as shown on the figure 20. But it is important to

compare these results with the frequency evolution of the directivity given on figure 12 to see the effects of the losses (\cong 3.2 dB). 2.6 dB are due to the power divider and 0.6 dB due to the connectors and cables.

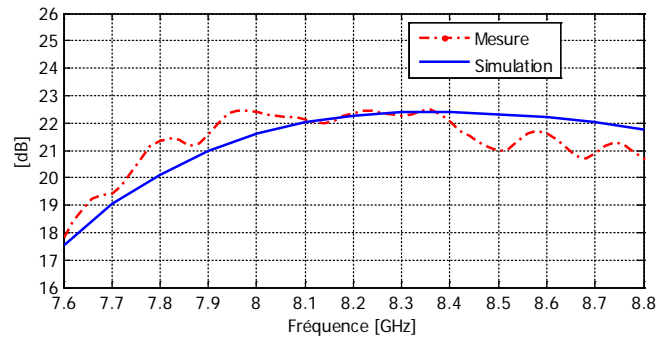


Fig. 20 Realized gain as a function of the frequency.

IV. CONCLUSION

This paper introduces a new approach called ARMA to build agile beam antenna and shows the differences with the well-known solution called AESA.

First the two electromagnetic principles are compared showing fundamental differences. The important performance shift illustrates the interest of the new approach but the manufacturing of ARMA is a little bit more complicate. However the cost is not significantly larger, because for such an antenna that is the BFN that set the price high or low and in the both antennas the same kind of BFN is used (sometimes with a lower number of elements for the ARMA solution).

ACKNOWLEDGMENT

The authors would like to thank Professor Raj Mittra which suggested this paper and Doctor Anthony Bellion for our helpful discussions.

REFERENCES

- [1] H. ABOU TAAM, G. ZAKKA EL NASHEF, M. SALAH TOUBET, E. ARNAUD, B. JECKO, T. MONEDIERE and M. RAMMAL
«Scan Performance And Reconfigurability Of Agile Radiating Matrix Antenna Prototype»
International Journal of Antennas and Propagation IJAP Vol. 2015 Article ID169303 8 pages. DOI : 10.1155:2015:169303.
- [2] Hussein ABOU TAAM, Moustapha SALAH TOUBET, Thierry Monedière, Bernard JECKO, Mohamed RAMMAL.
«A New Agile Radiating System Called Electromagnetic Band Gap Matrix Antenna»
Journal: International Journal of Antennas and Propagation, vol. 2014, Article ID 342518, 7 pages, 2014.
- [3] JECKO, B.; HAJI, M.; CHANTALAT, R.. SALAH TOUBET, M.
«Antenne élémentaire et antenne réseau mono ou bidimensionnelle correspondante»
PCT Patent: PCT/EP2012/076509; French Patent: FR 11 62141
- [4] Hussein ABOU TAAM, Moustapha SALAH TOUBET, Thierry MONEDIERE, Bernard JECKO, Mohamed RAMMAL.
«L'intérêt de la Matrice BIE 1D par rapport au Réseau des Patchs en termes de Couplage Mutuel et de Lobes Réseaux»
17eme Journées Nationales Microondes, 15-17 Mai 2013, Paris, France.
- [5] L. SCHWARTZ

- « Methode mathématiques pour les sciences physiques»
Collection Enseignement des Sciences – Hermann – Oct. 1997.
- [6] Hussein ABOU TAAM, Georges ZAKKA EL NASHEF, Moustapha SALAH TOUBET, Eric ARNAUD, Bernard JECKO, Mohamed RAMMAL.
«Feeding technique for the experimental validation of EBG matrix antenna»
Journal: Microwave and Optical Technology Letters, Vol 57, n°3, March 2015, Article ID MOP-14-0936.
- [7] Hussein ABOU TAAM, Moustapha SALAH TOUBET, Thierry MONEDIERE, Bernard JECKO, Mohamed RAMMAL «Interests of a 1D EBG Matrix compared to a patch array in terms of mutual coupling and grating lobe»
IEEE, 7th European Conference on Antennas and Propagation EuCAP, 8-12 April 2013, Sweden.
- [8] C. MENUDIER, M. THEVENOT, T. MONEDIERE, B. JECKO
«EBG Resonator Antennas : State of Art and Prospects»
6th International Conference on Antenna Theory and Techniques ICATT'07, Sevastopol, the Crimea, Ukraine, September 17-21, 2007.
- [9] Ali SIBLINI, Bernard JECKO, Hussein ABOU TAAM, Mohamed RAMMAL
«New Circularly Polarized Matrix Antenna For Space Applications»
WTS 2016 - London – 18/04/2016 au 20/04/2016.
- [10] Hussein Abou Taam, Georges Zakka El Nashef, Eric Arnaud, Nicolas Chevalier, Bertrand Lenoir, Bernard Jecko, Mohamed Rammal
«Design Development And Experimental Validation Of An EBG Matrix Antenna For Tracking Application»
International Journal of Microwave and Wireless Technology IJMWT : page 1 of 9 Cambridge University Press and European Microwave Association 2015
- [11] Hussein Abou Taam, Ali Siblani, Georges Zakka El Nashef, Bernard Jecko, Eric Arnaud, Nicolas Chevalier, Mohamed Rammal
«An Agile Electronically Scanned EBG Matrix Antenna For Monitoring Target Activity»
EUMW-EURAD (Paris 2015)
XLIM OSA (Ondes et Systèmes Associés) Limoges University - Limoges, France – GRIT Dept. -Lebanese University Beirut, Lebanon
- [12] Toubet, M.S.; Hajj, M.; Chantalat, R.; Arnaud, E.; Jecko, B.; Monediere, T.; Hongjiang Zhang; Diot, J.,
«Wide Bandwidth, High-Gain, and Low- Profile EBG Prototype for High Power Applications»
Antennas and Wireless Propagation Letters, IEEE , vol.10, no., pp.1362,1365, 201
- [13] Moustapha SALAH TOUBET, Hussein ABOU TAAM, Régis Chantalat, Bernard JECKO, Jean Christophe DIOT.
«Prototype d'une Antenne BIE Ultra Low-profile, Large Bande et Grand Gain pour des Applications de Forte Puissance»
17eme Journées Nationales Microondes, 15-17 Mai 2013, Paris, France.

and now for Telecommunications, Radar, and Electronic Warfare applications. He created and headed the department OSA (Ondes et Systèmes Associés – Waves and associated systems) at the XLIM institute: University of Limoges – CNRS laboratory until 2009. In January 2009, he was appointed as a DRRT (Regional Delegate for Research and Technology) by the French Research Ministry until his retirement in September 2013. Since then, he is coming back to his research department as an Emeritus Professor where he completes the supervision of a thesis in collaboration with a public Lebanese university and he was retained for another three years as a supervisor of a new thesis. Publications \cong 130 – Communications \cong 400 - Patents \cong 30 – Thesis supervision \cong 130 – HDR \cong 7



B. Jecko was born in Tréllissac (24), France in 1944. He obtained the Ph.D. degree in physics from the University of Limoges (France) in 1979. In this university, he served as a professor (exceptional class in 2000) at the IUT (GE teaching department founder in Brive in 1985), at the Electrical Engineering School ENSIL and at the Faculty of Sciences of Limoges until 2009. In the research area he was an electromagnetism specialist for EMC (fellow member EMP)